Mechatronics 22 (2012) 45–54

Contents lists available at SciVerse ScienceDirect

Mechatronics

journal homepage: www.elsevier.com/locate/mechatronics

Improved transparency in energy-based bilateral telemanipulation

Michel Franken *, Sarthak Misra, Stefano Stramigioli

Control Engineering Group, MIRA – Institute for Biomedical Technology and Technical Medicine, University of Twente, 7500 AE Enschede, The Netherlands

ARTICLE INFO

Article history:
Received 6 December 2010
Accepted 8 November 2011
Available online 9 December 2011

Keywords:
Telemanipulation
Bilateral control
Stability
Passivity
Transparency

ABSTRACT

In bilateral telemanipulation algorithms based on enforcing time-domain passivity, internal friction in the devices poses an additional energy drain. This can severely decrease the obtainable transparency of these algorithms when high amounts of friction are present in the slave device. Based on a model of the friction, the dissipated energy can be estimated and reclaimed inside the energy balance of the control algorithm. Extending the energy balance which is monitored, decreases the net passivity of the telemanipulation system enforced by the control algorithm, which usually enforces passivity of just the bilateral controller. Experimental results are provided that demonstrate the effectiveness of the proposed approach in increasing the obtainable transparency. As long as the physically dissipated energy is underestimated, the telemanipulation system as a whole will remain passive. Thus the guaranteed stability property of the time-domain passivity algorithm is maintained.

1. Introduction

A bilateral telemanipulation system presents the user with haptic feedback about the interaction between the slave device and the remote environment. The transparency of the telemanipulation system is defined as the degree to which it is able to convey to the user the perception of direct interaction with the environment [1]. One of the factors that determine the achievable transparency is the implemented bilateral control algorithm. Various control algorithms for bilateral telemanipulation have been proposed/applied with different stability and transparency properties, amongst others Position-Force controllers e.g. [2], Four Channel control [1], Impedance Reflection algorithms e.g. [3], and Coupled Impedance controllers, e.g. [4]. A recent overview can be found in [5].

Stability issues can arise in bilateral telemanipulation systems due to e.g. hard contacts in the environment and time delays in the communication channel connecting the master and slave system. The concept of passivity is often used in the design of bilateral telemanipulation systems as the interaction between passive systems is guaranteed to be stable. Both the user and the environment can be assumed to be passive, or to interact at least with passive systems in a stable manner [6]. Thus guaranteeing passivity of the telemanipulation system ensures stability of the interaction between the user/environment and the telemanipulation system.

Non-linear control architectures have been proposed in literature that can be combined with regular bilateral control algorithms to ensure passivity of the system. These algorithms adapt the commanded forces computed by the bilateral control algorithm to ensure that the telemanipulation system remains passive. Due to the adaptation of the command signals the interaction with this system is guaranteed to be stable, even though the bilateral control algorithm itself would result in unstable behavior of the system. Examples include the work of Ryu et al. [7,8], Kim and Ryu [9], Lee and Huang [10], and Franken et al. [11]. Of these approaches we will focus on Time Domain Passivity (TDP) algorithms, e.g. [7,8,11]. In TDP algorithms an energy balance of the system is monitored. This balance is based on the energy exchange between the physical world and the bilateral control algorithm. Passivity of that interaction is enforced with modulated dampers.

Perfect transparency means that the user should not be able to discern the dynamic behavior of the mechanical master and slave device, and the bilateral control algorithm during operation. When left uncompensated, mechanical friction at both the master and slave side can decrease the obtained transparency [12]. In this paper we will consider bilateral telemanipulation systems that consist of impedance-type displays (force output causality). For such devices mechanical friction can decrease the tracking performance with respect to the desired position at the slave side and the desired force at the master side. At the master side the mechanical friction will distort the force feedback experienced by the user, which is most apparent during free space motion.

Extensive research has been performed with respect to friction compensation in motion and force control. Methods have been proposed that use observer-based compensators, e.g. [13,14], adaptive controllers, e.g. [15,16] force feedback control, e.g. [17,18], and model-based feedforward compensation, e.g. [19–22]. Overviews of various sources of friction, applicable models and various

* Corresponding author.
E-mail addresses: m.c.j.franken@utwente.nl (M. Franken), s.misra@utwente.nl (S. Misra), s.stramigioli@utwente.nl (S. Stramigioli).

0957-4158/$ - see front matter © 2011 Elsevier Ltd. All rights reserved.
doi:10.1016/j.mechatronics.2011.11.004

compensation methods applied to systems with friction are published by Armstrong-Hélouvry et al. [23] and Bona and Indri [24].

Examples of friction compensation specifically applied to bilateral telemanipulation systems and haptic feedback devices include the work of Kwon and Woo [17], Bernstein et al. [18], Bi et al. [25], and Mahvash and Okamura [21]. Mahvash and Okamura [21] discuss that not every compensation method is suitable to be applied in bilateral telemanipulation systems depending on the chosen bilateral control algorithm and available sensors.

So far the effect of physical friction on the performance of TDP algorithms has been mostly neglected. Monfaredi et al. [26] recognized that TDP algorithms provide better results when applied to lightweight devices with low internal friction. Increased amounts of internal friction in the slave device were found to reduce the obtainable transparency with the telemanipulation system. Therefore they proposed to apply a stiffness observer to the interaction with the environment and make the damping applied at the user side dependent on the identified stiffness instead of the energy balance when slave devices with higher internal friction are used. In their approach the energy balance is no longer monitored, making the approach similar to the one proposed by Love and Book [27]. However, the required amount of damping to enforce passive behavior of the system is not solely dependent on the stiffness of the environment, e.g. the influence of the grasp of the user, the parameters of the bilateral controller, the device impedances, and the type of motion is neglected. Furthermore, the stability properties of the system become dependent on the convergence of the applied stiffness identification algorithm. Although an interesting approach, it fails to address the underlying problem of TDP algorithms.

In this paper, the influence of friction on TDP algorithms is analyzed. The analysis is performed based on the two-layer framework introduced by Franken et al. [11]. It will be shown that friction influences the system in two distinct ways, which can each be separately handled in one of the layers. In the *Transparency Layer* one of the aforementioned compensation methods can be applied to increase the performance with respect to motion and force tracking. In the *Passivity Layer* an energy-based compensation method is proposed. The focus of the paper lies on this last compensation method. Furthermore, the proposed approach is applicable in any TDP algorithm, e.g. [7,8]. A preliminary analysis and simulation results of this improvement in obtainable transparency was presented by Franken et al. [28]. The contribution of this paper are the extended analysis of the proposed friction compensation technique in the monitored energy balance of the TDP algorithm and its experimental validation.

The paper is organized as follows: Section 2 introduces the two-layer approach to bilateral telemanipulation. Section 3 discusses the influence of friction within the two-layer framework and the proposed compensation strategy. Section 4 describes an implementation of such a friction compensation technique in the two-layer framework. Experimental results with this implementation showing the obtainable increase in transparency are presented in Section 5. A discussion on the proposed approach is contained in Section 6. The paper concludes and provides direction for future work in Section 7.

2. Two-layered bilateral telemanipulation

In this section we will summarize the working of the two-layered framework proposed by Franken et al. [11].[1] Two layers are defined that each address a distinct goal. The *Transparency Layer* contains the bilateral control algorithm that makes the system display the desired behavior, whereas the *Passivity Layer* enforces passivity of the system, see Fig. 1.

The *Transparency Layer* can contain any control algorithm that delivers the desired transparency, as long as it results in a desired torque/force to be applied to the devices at both sides, e.g. [1–4]. The generalized forces to be applied at the master and slave side are τ_{TLm} and τ_{TLs}, respectively. These desired forces are the inputs to the *Passivity Layer* of which the working is summarized below.

A system is passive when the energy that can be extracted from the system is bounded by the energy that was injected into the system and the energy initially stored in the system, $E(0)$:

$$\int_{t_0}^{t_1} -\tau_I(t)\dot{q}_I(t)dt \geqslant -E(0), \tag{1}$$

where τ_I and $\dot{q}_I$ are the force and velocity associated with the interaction point of the system. $E(0)$ is assumed to be zero. Non-passive systems are said to generate "virtual" energy and it is this additional energy that can potentially destabilize the system.

For impedance-type systems (force output causality) the energy exchange between the control system and the physical world during sample period $\bar{k}$, ΔH_I, (k) can exactly be determined *a posteriori* as:

$$\begin{aligned}\Delta H_I(k) &= \int_{(k-1)\Delta T}^{k\Delta T} -\tau_I(t)\dot{q}_I(t)dt \\ &= -\tau_I(\bar{k})\int_{(k-1)\Delta T}^{k\Delta T} \dot{q}_I(t)dt \\ &= -\tau_I(\bar{k})\Delta q_I(k),\end{aligned} \tag{2}$$

where $\Delta q_I(k)$ is the position difference of the interaction point that occurred during sample period $\bar{k}$. Using (1) and (2) an energy balance, H_T, of the bilateral controller can be composed as

$$\begin{aligned}H_T(\bar{k}) &= \int_{t_0}^{t_1} -\tau_{PLm}(t)\dot{q}_M(t) - \tau_{PLs}(t)\dot{q}_S(t)dt \\ &= \sum_{i=0}^{(k-1)\Delta T} \Delta H_{Im}(i) + \Delta H_{Is}(i),\end{aligned} \tag{3}$$

where τ_{PLm} and τ_{PLs} are the forces exerted by the *Passivity Layer* on the master and slave device, respectively. The velocities of the master and slave device are $\dot{q}_M$ and $\dot{q}_S$, respectively. $\Delta H_{Im}(k)$ and $\Delta H_{Is}(k)$ are computed according to (2) and represent the energy exchanged between the physical world and the control system, operating in discrete time, at the master and slave side, respectively. (3) represent the amount of energy 'stored' in the bilateral control algorithm. If (3) is enforced to be positive always, the telemanipulation system is passive and thus stability will be guaranteed.

To account for time delays in the communication channel the *Passivity Layer* splits (3) into three parts:

$$H_T(\bar{k}) = H_M(\bar{k}) + H_C(\bar{k}) + H_S(\bar{k}), \tag{4}$$

where H_M, H_C, and H_S represent the energy at the master side, in the communication channel, and at the slave side. The energy at the master and slave side, H_M and H_S, are stored in energy tanks. The energy levels in these tank can be regarded as energy budgets from which controlled movements can be powered. An energy transfer protocol is required to make energy available in the system where needed. An example is the Simple Energy Transfer Protocol (SETP), where each side transmits each iteration a fraction, β, of its energy level to the other side. This guarantees $H_C \geqslant 0$ for arbitrary time delays and ensures asymptotic stability of the difference of the tank levels for arbitrary constant time delays. The proof of the latter is obtained by a straightforward application of the Jury Stability

[1] With respect to the mathematical notation used in this paper we would like to point out the following. The index k is used to indicate instantaneous values at the sampling instant k and the index $\bar{k}$ is used to indicate variables related to an interval between sampling instants $k-1$ and k. The symbol τ is used to indicate a generalized force vector which can contain both forces and torques.

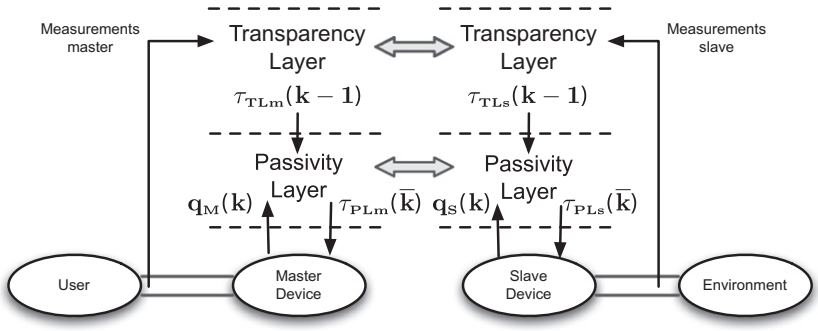

Fig. 1. Two layer algorithm for bilateral telemanipulation. The double connections indicate an energy exchange interaction [11].

Criterion to the linear time invariant description of the tank level difference.

With the SETP there are three energy flows connected to each energy tank, the energy exchange that occurs with the physical world and both an incoming and outgoing energy flow from the communication channel. The energy tank levels are given as

$$\begin{aligned} H_M(\bar{k}) &= \sum_{i=0}^{(k-1)\Delta T} \Delta H_{Im}(k) + \Delta H_{SM+}(k) - \Delta H_{MS-}(k) \\ H_S(\bar{k}) &= \sum_{i=0}^{(k-1)\Delta T} \Delta H_{Is}(k) + \Delta H_{MS+}(k) - \Delta H_{SM-}(k), \end{aligned} \tag{5}$$

where ΔH_{MS-} and ΔH_{MS-} are the energy packets send each iteration into the communication channel at the master and slave side. ΔH_{MS+} and ΔH_{SM+} are the amounts of energy received at each side out of the communication channel. The energy flow out of the communication channel at each side is the time-delayed energy flow into the communication channel at the other side. A thorough treatment of the two-layer framework is contained in [29].

When the energy level at either the master or slave side is low, the force that can be exerted by the bilateral control algorithm at that side is restricted to maintain passivity. Saturation functions can be implemented that guarantee

$$\begin{aligned} &H_M(\bar{k}) \geqslant 0 \\ &H_S(\bar{k}) \geqslant 0. \end{aligned} \tag{6}$$

Examples of such saturation functions are discussed in [11]. The various saturation functions that are implemented compute maximum torques, $\tau_{Mmax}(k)$ and $\tau_{Smax}(k)$ that can be applied at the master and slave side by the *Passivity Layer* during sample period $\overline{k+1}$ so that passivity will be maintained. The forces applied by the *Passivity Layer* are computed as

$$\begin{aligned} \tau_{PLm}(\overline{k+1}) &= \operatorname{sgn}(\tau_{TLm}(k)) \min(|\tau_{TLm}(k)|, \tau_{Mmax}(k)) + \tau_{TLC}(k) \\ \tau_{PLs}(\overline{k+1}) &= \operatorname{sgn}(\tau_{TLs}(k)) \min(|\tau_{TLs}(k)|, \tau_{Smax}(k)), \end{aligned} \tag{7}$$

where τ_{TLC} is the force exerted by the Tank Level Controller (TLC). The TLC is defined at the master side to regulate the energy level in the system independent of the bilateral control algorithm in the *Transparency Layer*. The TLC is activated in order to extract an initial amount of energy, and further additionally required energy, from the user to maintain a desired energy level in the system. The TLC is implemented as a modulated viscous damper:

$$\begin{aligned} &\tau_{TLC}(k) = -d(k)\dot{q}_M(k) \\ &d(k) = \begin{cases} \alpha(H_D - H_M(\overline{k+1})) & \text{if } H_M(\overline{k+1}) < H_D \\ 0 & \text{otherwise} \end{cases}, \end{aligned} \tag{8}$$

where H_D is the desired energy level of the tank and $d(k)$ is the modulated viscous damping coefficient and α is a tuning parameter for the rate at which the user will replenish the energy tank given a certain motion. The selection of H_D and α dependents on the device characteristics, the implemented energy transfer protocol, and the properties of the communication channel [29]. Systematic tuning of the parameters in the *Passivity Layer* is the topic of ongoing research.

The algorithm implemented in the *Passivity Layer* maintains the energy balance:

$$H_T(\bar{k}) = \sum_{i=0}^{k-1} \Delta H_{Im}(i) + \Delta H_{Is}(i) \geqslant 0, \tag{9}$$

which guarantees passivity of the bilateral control algorithm and thus of the telemanipulation system as a whole.

3. Friction

In the previous section the two-layer approach to bilateral telemanipulation was described. In this section the influence of friction on the performance of each layer will be analyzed. It will be shown that in each layer compensation methods of a different nature need to be implemented to achieve the highest possible level of transparency while guaranteeing stability.

3.1. Transparency Layer

The bilateral control algorithm in the *Transparency Layer* is intended to provide the user with the desired level of transparency. For most bilateral control algorithms this translates into the following goals:

- accurate reflection of the environment force to the user,
- accurate position tracking by the slave device with respect to the motion of the master device.

Mechanical friction in the master and slave device can reduce the performance of the system with respect to these two goals. The rigid-body dynamic equations of the master and slave system are:

$$\begin{aligned} \tau_{PLm}(t) + \tau_H(t) + \tau_{Rm}(t) &= M_M(q_M)\ddot{q}_M(t) \\ \tau_{PLs}(t) + \tau_E(t) + \tau_{Rs}(t) &= M_S(q_S)\ddot{q}_S(t), \end{aligned} \tag{10}$$

where τ_H and τ_E are the forces exerted by the user and the environment, respectively. τ_{Rm} and τ_{Rs} are the non-linear mechanical friction forces in the master and slave device and M_M and M_S are the configuration dependent inertia matrices of the master and slave device, respectively.

In order to achieve the desired goals τ_{TLm} and τ_{TLs} need to be designed such that the negative influence of friction, τ_{Rm} and τ_{Rs}, with respect to the desired goal is removed. If force/torque sensors are available force feedback control can be applied at the master side,

e.g. [17]. If a sufficiently accurate model of the friction can be derived, model-based feedforward control can be applied, e.g. [19]. Bernstein et al. [18] conclude that a hybrid implementation of these two approaches offers superior performance when compared to the performance of the separate approaches. At the slave side, an adaptive position controller can be used to change the parameter gains to achieve a desired measure of position tracking, e.g. [16], or model-based feedforward control can be applied to obtain the same goal, e.g. [21]. Mahvash and Okamura [21] discuss that for a position-position control architecture, adaptive techniques based on a pure position tracking error cannot be applied as the tracking error is also influenced by the interaction with the environment. Force-feedback control cannot be applied as the slave device can also be operating in free space.

3.2. Passivity Layer

The algorithm described in Section 2 guarantees stability of the telemanipulation system by enforcing passivity of the bilateral control algorithm, (9). The rigid-body dynamic equations of (10) can be transformed into energy balances as:

$$\begin{aligned}\int_{(k-1)\Delta T}^{k\Delta T} -\tau_{PLm}(t)\dot{q}_M(t)dt &= \int_{(k-1)\Delta T}^{k\Delta T} (\tau_H(t) + \tau_{Rm}(t) \\ &\quad - M_M(q_M)\ddot{q}_M(t))\dot{q}_M(t)dt\Delta H_{Im}(k) \\ &= -\Delta H_H(k) - \Delta H_{Rm}(k) - \Delta H_{Km}(k), \end{aligned} \tag{11}$$

where $\Delta H_H(k)$, $\Delta H_{Km}(k)$ and $\Delta H_{Rm}(k)$ are the amount of energy exchanged between the master system and the user, the change of kinetic energy in the master device, and the energy dissipated due to friction in the master device during sample period $\bar{k}$. Similarly for the slave device:

$$\Delta H_{Is}(k) = -\Delta H_E(k) - \Delta H_{Rs}(k) - \Delta H_{Ks}(k), \tag{12}$$

where $\Delta H_E(k)$, $\Delta H_{Ks}(k)$ and $\Delta H_{Rs}(k)$ are the amount of energy exchanged between the slave system and the environment, the change of kinetic energy in the slave device, and the energy dissipated due to friction in the slave device during sample period $\bar{k}$. The signs in (11) and (12) are due to the definition of the positive energy flow direction according to (10).

It immediately follows from (12) that physical friction in the slave device not only influences the position tracking performance of the slave device, but also the energy balance as enforced by the *Passivity Layer*. This influence is independent of possible friction compensation methods implemented in the *Transparency Layer* to achieve proper position and force tracking. Consider the situation where the slave device is moving at a constant velocity in free space ($\Delta H_E(k) = 0$ and $\Delta H_{Ks}(k) = 0$). The energy balance of (12) reduces to:

$$\Delta H_{Is}(k) = -\Delta H_{Rs}(k). \tag{13}$$

This means that due to (9) the energy dissipated in the slave device will have to be injected by the user. As the slave device is moving in free space it is likely to assume that the commanded torque/force by the control algorithm in the *Transparency Layer* at the master side is zero, $\tau_{TLm}(k) = 0$. Therefore, the TLC will be activated so that the user injects energy into the system to compensate for ΔH_{Rs}. Subsequently, due to the activation of the TLC the user will not experience free space motion as such.

Similar arguments can be applied to the master system. Consider the situation where the user is moving at a constant velocity and that at the slave side $\Delta H_{Is}(k) = 0$. Assume that the user needs to experience free space motion ($\Delta H_H(k) = 0$) and that adequate friction compensation techniques have been applied in the *Transparency Layer* to achieve that free space motion sensation. From (11) it follows that:

$$\Delta H_{Im}(k) = -\Delta H_{Rm}(k), \tag{14}$$

which means that without additional measures in the *Passivity Layer* the TLC will again be activated. It can also be argued that without friction compensation in the *Transparency Layer* the user is injecting energy into the system to overcome the friction in the master device, ΔH_{Rm}, which can be used as partial fulfillment of the energy that would need to be extracted by the TLC.

A sufficient condition for stability of the telemanipulation system is that no energy can be extracted from the system as a whole, meaning that

$$\int_{t_0}^{t_1} \tau_H(t)\dot{q}_M(t) + \tau_E(t)\dot{q}_S(t)dt \geqslant 0. \tag{15}$$

By implementing the *Passivity Layer* as described in Section 2, passivity of the bilateral controller is enforced. This means that (15) becomes

$$\int_{t_0}^{t_1} \tau_H(t)\dot{q}_M(t) + \tau_E(t)\dot{q}_S(t)dt \geqslant H_{Rm}(t_1) + H_{Rs}(t_1), \tag{16}$$

where $H_{Rm}(t_1)$ and $H_{Rs}(t_1)$ are the energy dissipated by friction in the master and slave device between t_0 to t_1, respectively. (16) indicates net passivity, which can be quite significant based on the amount of physical friction present in the master and slave device. This leads to the conclusion that the implementation of the *Passivity Layer* of Section 2 and TDP approaches in general are conservative as more friction is added to the system than strictly necessary to guarantee passivity of the telemanipulation system as a whole.

A solution to this conservatism in the *Passivity Layer* is to account for the dissipated energy in the monitored energy balance. Assume that a model of the friction in the master and slave device is available. Based on the implemented models and the position measurements, the amount of energy dissipated by friction during each sample period in the devices can be estimated. This would yield $\Delta\widetilde{H}_{Rm}(k)$ and $\Delta\widetilde{H}_{Rs}(k)$ at the master and slave side. Any model that is suitable to describe the friction can be implemented, see e.g. [23] for an overview of various models.

In the *Passivity Layer* the estimated amounts of energy are subsequently added to the energy tanks. This is sketched in Fig. 2 for the slave side. The energy balance that is enforced by the two-layer framework becomes:

$$H_T(\bar{k}) = \sum_{i=0}^{k-1} \Delta H_{Im}(i) + \Delta\widetilde{H}_{Rm}(i) + \Delta H_{Is}(i) + \Delta\widetilde{H}_{Rm}(i) \geqslant 0. \tag{17}$$

This prevents the TLC from being activated to compensate for the energy dissipated internally in the master and slave device, which would result in net passivity of the system. Stability is still guaranteed as the telemanipulation system as a whole remains passive according to (15). The only requirement to achieve (15) is

$$\sum_{i=0}^{k} \Delta\widetilde{H}_{Rm}(i) + \Delta\widetilde{H}_{Rs}(i) \leqslant \int_{t=0}^{k\Delta T} -\tau_{Rm}(t)\dot{q}_M(t) - \tau_{Rs}(t)\dot{q}_S(t), \tag{18}$$

which simply means that the estimate of the dissipated energy should be smaller than the physically dissipated energy so that a small amount of net passivity remains in (15).

An important difference with the friction compensation method in the *Transparency Layer* is that friction compensation in the *Passivity Layer* does not directly result in a force to be applied to the physical device. Assume that a model-based feedforward compensation method is implemented in the *Transparency Layer*. The computed feedforward force is physically applied to the device and will as such influence the motion of the device directly. The performance of friction compensation methods in the *Transparency Layer* can be reduced due to e.g. ignored non-linear effects such as stiction, the Stribeck effect, stick–slip, measurement noise, and

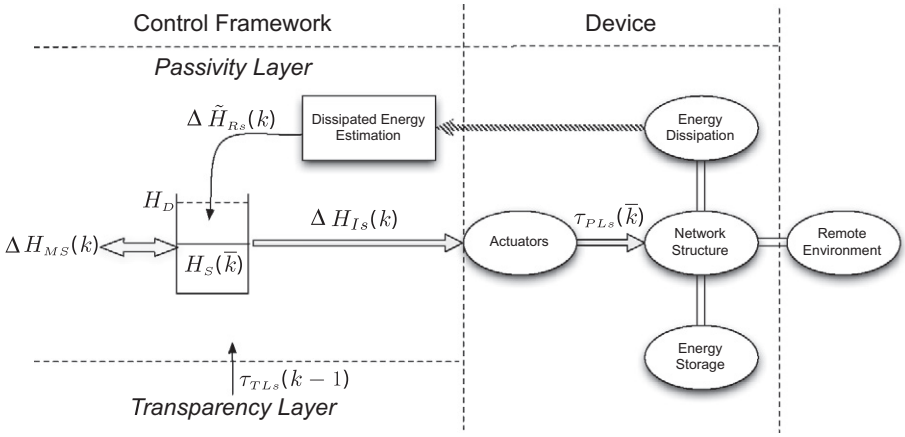

Fig. 2. Dissipated energy compensation at the slave side in the *Passivity Layer*: For clarity only the energy flows are depicted in the *Passivity Layer*, $\Delta H_{MS}(k)$ represents the energy exchange between the master and slave system through the communication network.

phase-lag due to possible filtering operations. These factors can significantly reduce the performance of the friction compensation method when the devices are moving at low velocities, especially near zero-crossings [25]. A possible consequence of such neglected effects is chattering of the device. By using more advanced compensation methods this can be mitigated, e.g. [30] where online identification and adaptation is used and [21] where a passive compensation method is implemented.

With respect to the friction compensation method in the *Passivity Layer* the only requirements are (18) and a certain smoothness of $\Delta\tilde{H}_{Rm}$ and $\Delta\tilde{H}_{Rs}$. Non-smoothness of $\Delta\tilde{H}_{Rm}$ and ΔH_{Rs} can cause non-smoothness in the TLC, which can be experienced by the user as disturbing. This means that the requirements on the competence of the model are much less strict in the *Passivity Layer* compared to the *Transparency Layer*. The inclusion of any friction model that adheres to these two conditions will reduce the net passivity of the telemanipulation system as enforced by the *Passivity Layer*. Thus the obtainable transparency will be increased by any such friction model.

A final aspect with respect to the proposed model-based friction compensation in the *Passivity Layer* that needs to be taken into account is the possible occurrence of a build up effect in the energy tanks. Consider the situation where the slave system is moving in free space, no friction compensation has been applied in the *Transparency Layer* at the master side, and perfect friction models are implemented in the *Passivity Layer*. Continuous compensation of the dissipated energy in the master device in the *Passivity Layer* will cause a build up effect. Energy is continuously added to the tank at the master side, $\Delta\tilde{H}_{Rm}(k) \geqslant 0$, whereas no energy is spend from the tank at the slave side, $\Delta H_{Is}(k) + \Delta\tilde{H}_{Rs}(k) = 0$. This build up effect will prevent the *Passivity Layer* from adequately suppressing unstable behavior of the telemanipulation system. The build up of energy will first have to dissipated by generated "virtual" energy that is associated with non-passive behavior of the bilateral control algorithm in the *Transparency Layer* before the *Passivity Layer* can stabilize the system. This means that the system can temporarily display unstable behavior due to this build up effect. This problem due to energy build up is associated with TDP algorithms in general and ad hoc resetting schemes have been proposed for the TDPC approach in e.g. [31,32]. It should be noted that the mentioned unstable behavior is actually potentially unstable behavior, as non-passive behavior (generation of "virtual" energy) is a required, but not sufficient condition for instability.

In the situation described above the build up effect in the *Passivity Layer* is caused by the continuous inclusion of the dissipated energy at the master side. For the compensation algorithm the circumstances need to be identified under which the dissipated energy can be safely compensated. Two possible methods are:

1. Always include $\Delta\tilde{H}_{Rs}(k)$ and only include $\Delta\tilde{H}_{Rm}(k)$ when $H_M(\bar{k}) < H_D$.
2. Only include $\Delta\tilde{H}_{Rs}(k)$ when $H_S(\bar{k}) < H_D$ and only include $\Delta H_{Rm}(k)$ when $H_M(\bar{k}) < H_D$.

where H_M, H_S, and H_D are again the energy levels of the tank at the master and slave side and the desired energy level for the tanks, respectively. The first approach is less conservative as more of the dissipated energy due to physical friction in the slave device is reclaimed in the energy balance enforced by the *Passivity Layer*. This approach is suitable to be applied under a forward energy-flow assumption, where motions can only be initiated by the user. If motions can be initiated from the environment a build up of energy in the *Passivity Layer* is still possible. The second strategy never leads to a build up of energy, but will result in a higher net passivity of the system to be enforced by the TDP algorithm due to the higher amount of neglected energy. Depending on the assumptions made about the environment one of these strategies should be selected.

4. Implementation

In this section the test setup used in the experiments will be introduced. A specific implementation of the two-layer framework will be presented along with an implementation of the proposed friction compensation method specific for the used test setup.

4.1. Test setup

The setup, Fig. 3, consists of two one degree of freedom devices powered by a DC motor without gearbox. The maximum continuous torque that these motors can exert is 1.38 Nm. A high-precision encoder with 65 k pulses per rotation is used to record the position of each device. The mechanical arms of the devices rotate in the plane parallel to the base plate. The mechanical arms contain a linear force sensor to record the force which is applied at the interaction point perpendicular to the arm in the plane of motion. The interaction point between the user/environment and the devices is at the end of each mechanical arm.

Both devices are controlled from the same controller running on a real-time Linux distribution. The controllers are implemented in the program 20-sim [33] and real-time executable code specific for this setup is generated directly from 20-sim and uploaded to the

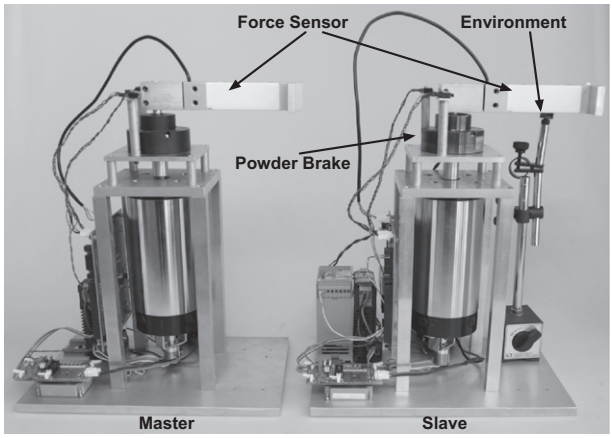

Fig. 3. Experimental setup: The setup consists of two one degree of freedom devices powered by an electromotor without gearbox. The position of each motor is recorded with a high-precision incremental encoder and the mechanical arm consists of a linear force sensor to record the interaction force between the user/environment and the devices. A powder brake is attached to the motor axis of the slave device which allows the amount of friction in the slave device to be controlled.

controller by means of the program 4C [33]. The sampling frequency of the control loop is 1 kHz. As environment a mechanical spring with a stiffness of approximately 1500 N/m is used. The recorded position of this spring in the environment varies slightly between experiments as only incremental position encoders are used and the initial position of the slave device is not perfectly equal for each experiment.

In order to demonstrate the effectiveness of the approach of Section 3 the level of friction in the slave device needs to be adjustable. To this end a powder brake (Merobel FAT 20) is incorporated in the slave device. A powder brake is essentially a bearing with a coil integrated in the component. When a current runs through the coil, the resulting electromagnetic field attracts ferromagnetic powder in between the running surfaces of the bearing creating coulomb friction. The amount of coulomb friction is approximately linearly dependent on the applied current.

4.2. Two-layer framework

In the *Transparency Layer* a regular Position-Force controller is implemented as given by:

$$\begin{aligned} \tau_{TLm}(k) &= rF_e(k) \\ \tau_{TLs}(k) &= K_p(q_M(k) - q_S(k)) - K_d\dot{q}_S(k) \end{aligned} \tag{19}$$

where F_e is the measured interaction force between the slave device and the environment, $r = 0.15$ m is the length of the mechanical arm of each device, and K_p and K_d are the proportional and derivative gain of the PD-type position controller, respectively.

The focus of this paper is the effect of friction compensation with respect to the obtainable transparency in the two-layer framework. The proposed approach of Section 3 consists of local procedures at the master and slave side. Due to this locality their performance is not dependent on possible time delays in the communication channel. Therefore, in this paper a non-delayed implementation is considered. In this non-delayed implementation the energy tanks in the *Passivity Layer* at the master and slave side, H_M and H_S, are merged into a single energy tank H_T. Furthermore, to show the effectiveness of the friction compensation no additional saturation functions have been implemented. This implementation of the two-layer framework is comparable to the standard TDPC algorithm as proposed by Ryu et al. [7] with a non-zero positive value to be maintained in the energy balance.

Table 1
Control structure parameter values.

Parameter	Value	Parameter	Value
K_p	3.75 Nm/rad	K_d	0.11 Nm s/rad
H_D	1 J	α	50 Nm s/rad J

The TLC is implemented as (8). Both the tuning parameter of the TLC and the tank level are chosen such that the energy tank is never depleted during normal operation for the various operating conditions of all experiments.

The parameters used for all elements of the control structure are listed in Table 1.

4.3. Friction compensation

Device identification experiments showed that the mechanical friction in the slave device can be approximated by coulomb friction and that the amount of viscous friction is negligible. The coefficient for the coulomb friction, $\widetilde{B}_C$ of the slave device was determined to be approximately 0.06 Nm, of which most is due to the residual torque of the powder brake. Actuation of the powder brake will increase the amount of coulomb friction in the slave device. Three different levels of friction added by the powder brake have been used. The estimated levels of coulomb friction in the slave device were low friction ($\widetilde{B}_C = 0.06$ Nm), medium friction ($\widetilde{B}_C = 0.4$ Nm), and high friction ($\widetilde{B}_C = 1$ Nm). The amount of friction in the master device is negligible.

It is chosen not to include friction compensation in the *Transparency Layer*. Due to mechanical play in the slave device, feedforward friction compensation based on a simple coulomb friction model, Fig. 4, causes chattering. The use of adaptive position controllers has also been neglected as the focus of this paper lies on the friction compensation applied in the *Passivity Layer*. This means that the position tracking performance of the slave device with respect to the master device will decrease when the amount of friction in the slave device is increased.

It is assumed that no movements can be initiated from the environment, so that continuous friction compensation in the *Passivity Layer* of $\Delta\widetilde{H}_{Rs}$ at the slave side can be implemented. As the friction in the master device is negligible no friction compensation is included in the *Passivity Layer* at the master side.

The coulomb friction model, Fig. 4, is given by

$$\tilde{\tau}_{Rs}(t) = -\widetilde{B}_C \mathrm{sgn}(\dot{q}_S(t)). \tag{20}$$

The energy dissipated, $\Delta\widetilde{H}_{Rs}(k)$, during a sample period, $\bar{k}$, can be computed *a posteriori* at sample instant k. The input for this compu-

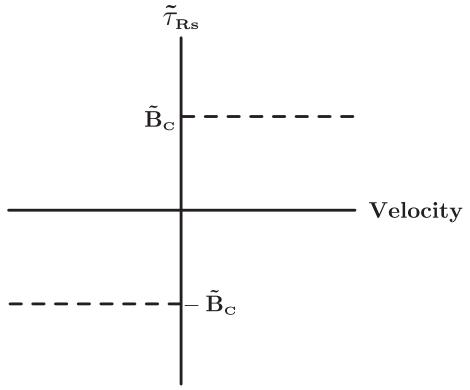

Fig. 4. Friction model: The used friction model consists purely of coulomb friction. The friction compensation technique can accommodate any type of friction model that (partially) describes the physical friction in the device.

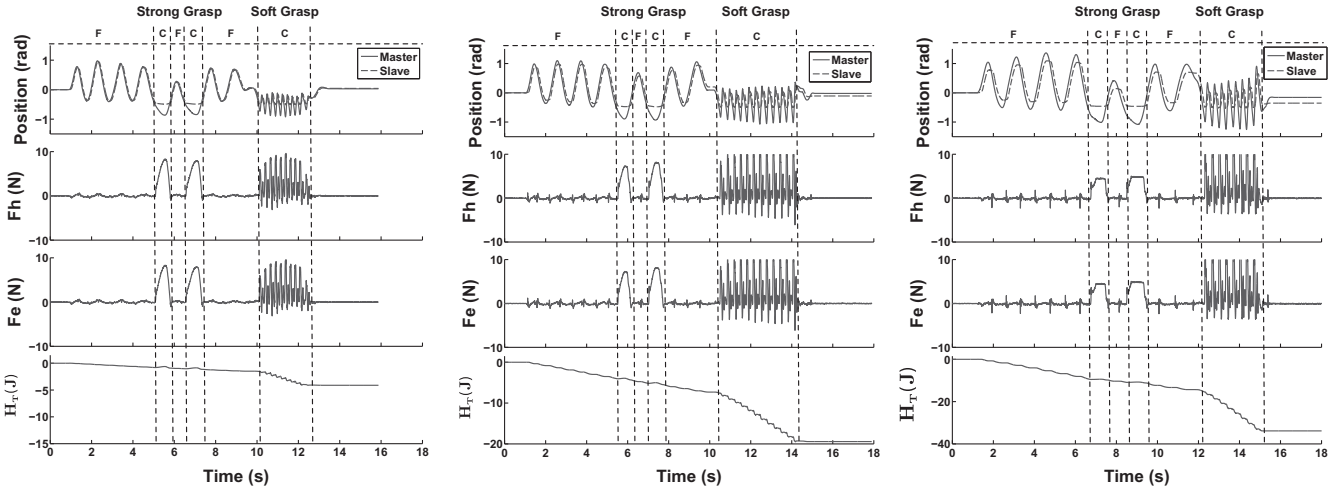

(a) Low friction (b) Medium friction (c) High friction

Fig. 5. Experimental results with *Passivity Layer* switched off: *F* and *C* indicate free space motion and contact phases, respectively. For all three friction levels excellent free space behavior is obtained, only inertial effects of the force sensor in the slave device are discernible in the feedback force to the user. However, this non-passive implementation results in an unstable interaction with the remote environment when the user applies a soft grasp.

tation is the displacement of the slave device that has occurred during the sample period, $\bar{k}$. As this computed energy is added to the energy tank in the *Passivity Layer* overestimation of the physically dissipated energy needs to be prevented. This not only concerns the used model parameters, but also the presence of possible measurement noise needs to be taken into account. Franken et al. [28] show how the energy function described below can be adjusted based on the stochastic characteristics of the measurement noise.

The estimated power, $\widetilde{P}_C(t)$, dissipated due to coulomb friction is

$$\widetilde{P}_C(t) = \widetilde{B}_C|\dot{q}_S(t)| \tag{21}$$

The integral of (21) during a sample period gives the estimated dissipated energy. However, it is not possible to detect a change of direction during a sample period. Therefore the estimated energy dissipated by the coulomb friction, $\Delta\widetilde{H}_{Rs}(k)$, directly from the measured displacement, $\Delta q_S(k)$, as

$$\Delta\widetilde{H}_{Rs}(k) = \widetilde{B}_C|\Delta q_S(k)| \leqslant \int_{(k-1)T}^{kT} B_C|\dot{q}_S(t)|dt \tag{22}$$

which is a lower-bound of the physically dissipated energy as long as $\widetilde{B}_C < B_C$, where B_C is the physical coulomb friction coefficient.

5. Experiments

In this section we will demonstrate that the compensation method of Section 3 increases the transparency obtainable with TDP algorithms. The stability properties of the TDP algorithm are unaffected as long as the used friction model underestimates the physical friction.

Three different levels of friction added by the powder brake were used. The estimated levels of coulomb friction in the slave device were low friction ($\widetilde{B}_C = 0.06$ Nm), medium friction ($\widetilde{B}_C = 0.4$ Nm), and high friction ($\widetilde{B}_C = 1$ Nm). These friction coefficients are

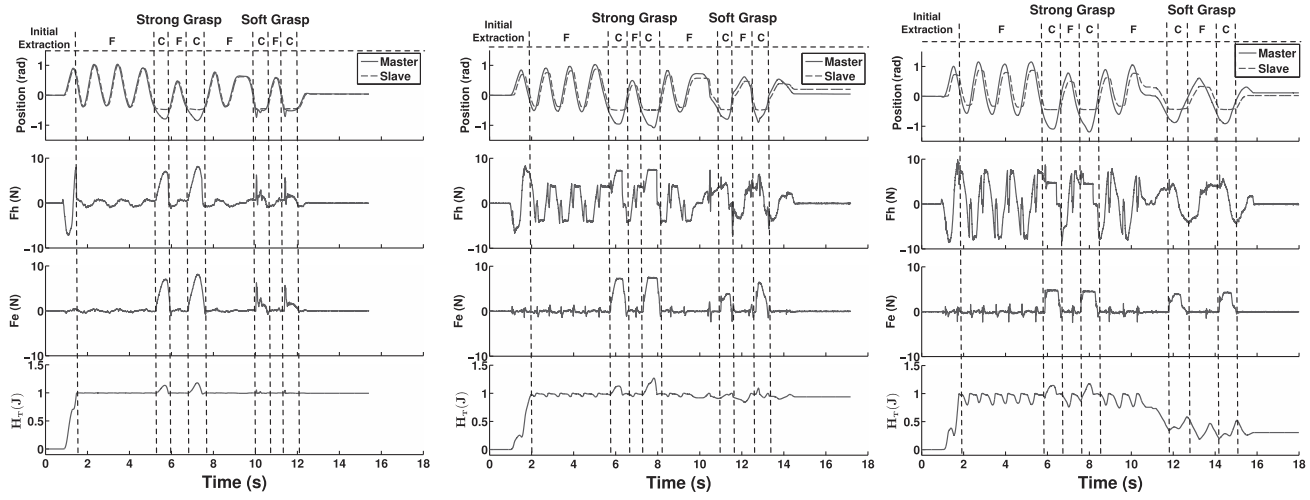

(a) Low friction (b) Medium friction (c) High friction

Fig. 6. Experimental results with standard *Passivity Layer*: *F* and *C* indicate free space motion and contact phases, respectively. The passivity condition which is enforced prevents instability of the interaction with the remote environment even when the user applies a soft grasp. However, for increasing friction levels in the slave device the transparency of the telemanipulation decreases due to the continuous activation of the *Passivity Layer*.

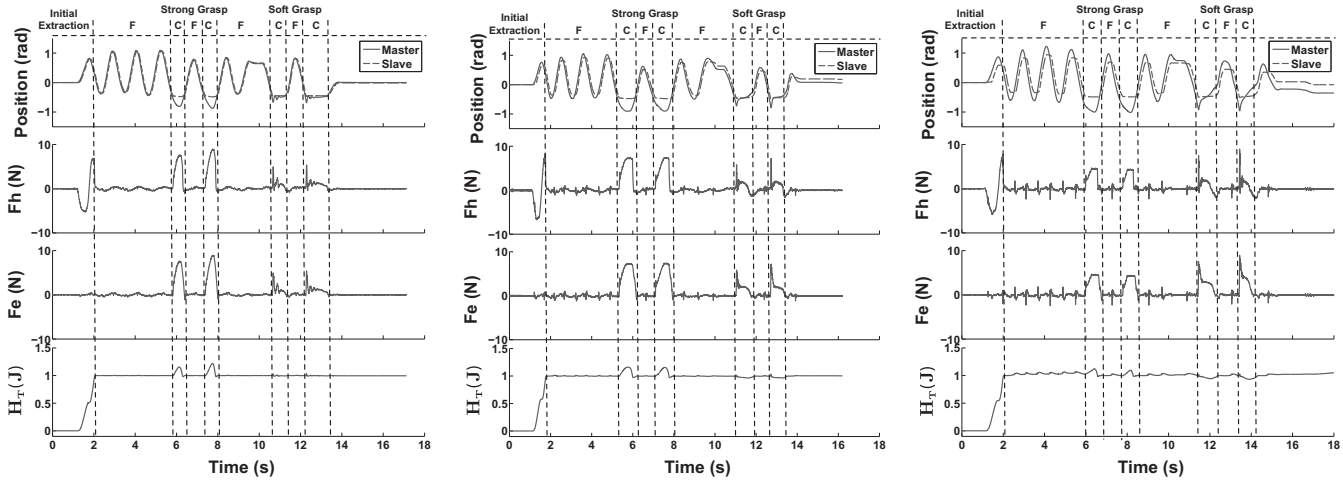

(a) Low friction (b) Medium friction (c) High friction

Fig. 7. Experimental results with extended *Passivity Layer*: *F* and *C* indicate free space motion and contact phases, respectively. Extending the energy balance in the *Passivity Layer* to incorporate the device friction reduces the conservatism of the algorithm. The user experiences free space motion even for high friction levels and stability of the interaction is still guaranteed even for a soft grasp by the user.

conservative enough so that the physically dissipated energy is not overestimated. The position controller at the slave device is not optimized to cope with increased amounts of friction in the slave device. This means that the position tracking performance will decrease when the friction is increased.

For all friction levels three different implementations of the *Passivity Layer* were tested:

- *Passivity Layer* switched off,
- regular *Passivity Layer*,
- extended *Passivity Layer* with friction compensation at the slave side.

During each experiment a repetitive motion pattern was carried out (movement in free space, 2 contact phases with a stiff user grasp, movement in free space, and finally 2 contact phases with a soft user grasp). During the stiff user grasp phase the user is firmly holding the device, whereas during the soft grasp phase the fingertips of the user are lightly touching the device. For each experiment the positions of the master and slave device are plotted together with the interaction forces between the user and the master device F_h and between the slave device and the environment F_e, and the level of the energy tank H_T in the *Passivity Layer*. Contact phases and free space motion are depicted by *C* and *F*, respectively.

Fig. 5 show the obtained results for the situation when the *Passivity Layer* is turned off. For all three friction levels excellent free space behavior is obtained, only the inertial effects of the force sensor are discernible in the feedback force to the user. The magnitude of these inertial effects increases for higher friction levels added by the powder brake due to stick–slip effects and the presence of a small amount of mechanical play in the slave device. Fig. 5 shows that the contact with the environment is unstable for a relaxed user grasp irrespective of the friction at the slave side.

When the standard *Passivity Layer* is activated, Fig. 6, these contact instabilities are prevented. However, a significant decrease in transparency is visible when the friction level in the slave device is increased. Already for the situation without additional friction supplied by the powder brake, Fig. 6a, an additional force is computed by the TLC in the *Passivity Layer* at the master side to maintain passivity of the monitored energy balance. This force is noticeable and the user does not experience free space motion as such. Finally, for higher amounts of friction the interaction force between the slave device and the environment is completely masked by the force added by the TLC. In this situation the user is not able to discriminate between contact phases and free space motion phases while moving the device. Only in static situations the user accurately experiences the interaction force between the slave device and the remote environment.

Fig. 7 shows the improvement in free space behavior when the standard *Passivity Layer* is extended with the friction compensation technique proposed in Section 3 and detailed in Section 4.3. The energy dissipated by the friction in the slave device is now estimated based on the identified coulomb friction model and added to the energy tank in the *Passivity Layer*. This means that the bilateral control algorithm is allowed to generate the energy that is needed to overcome the device friction. Non-passive behavior that could potentially destabilize the system is still suppressed by the *Passivity Layer*. This is demonstrated by the stability of the contact phases for both grasps by the user.

Fig. 7 shows that the extension to the *Passivity Layer* proposed in Section 3 can increase the transparency of the TDPC algorithm. This effect is especially noticeable during free space motion and is obtained by incorporating a model-based feedback loop in the *Passivity Layer*. However, the use of a model means that the energy balance is no longer solely based on measured energy exchanges, but also on an estimated quantity (the dissipated energy). When this model overestimates the physically dissipated energy, the TDP algorithm no longer guarantees passivity as "virtual" energy is generated in the established feedback loop. This is demonstrated in Fig. 8 where the friction coefficient used in the model, $\widetilde{B}_C = 0.24$ Nm is chosen four times larger as physically present, $B_C \approx 0.06$ Nm. A build up of energy occurs during free space motion. This excess energy in the energy-balance prevents the *Passivity Layer* from acting immediately on non-passive behavior of the bilateral controller in the *Transparency Layer* and results in momentary unstable behavior when the user applies a soft grasp. The *Passivity Layer* stabilizes the interaction as soon as the "virtual" energy generated by the non-passive behavior of the *Transparency Layer* has dissipated the "virtual" energy generated in the model-based feedback loop. This shows that a transparency versus stability trade-off is present in TDP algorithms. The transparency of the approach can be increased by incorporating more knowledge about the physical devices, but at the cost of robustness against modeling errors.

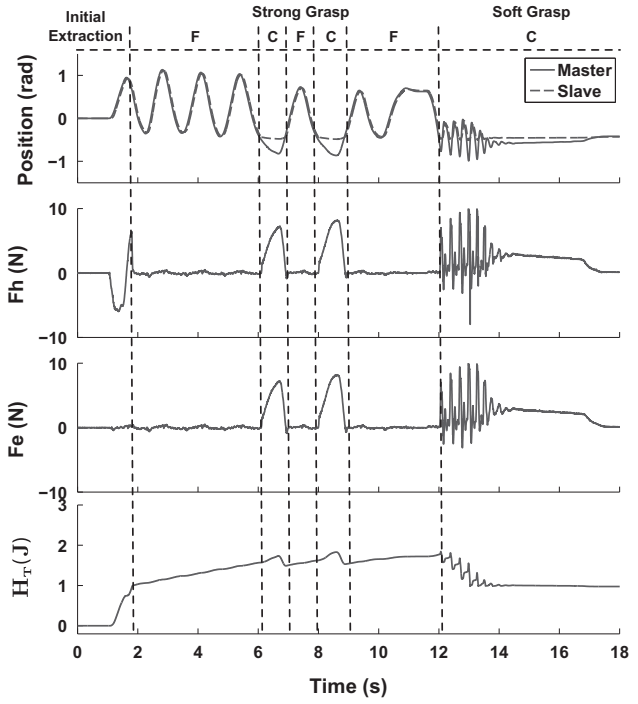

Fig. 8. Effect of overestimating dissipated energy: *F* and *C* indicate free space motion and contact phases, respectively. During free space motion "virtual" energy is generated in the model-based feedback loop which results in a rising level of the energy tank. This build up of energy prevents the *Passivity Layer* from acting immediately on non-passive behavior of the system, which can result in temporary unstable behavior.

6. Discussion

In Section 3 it was discussed that in order to obtain the highest possible transparency friction compensation has to be included in both the *Transparency*- and *Passivity Layer*. It could be argued that this can be circumvented by compensating for friction outside the two-layer framework. In Section 3.1 force feedback control and model-based feedforward control were indicated as possible friction compensation techniques suitable for application at the master side. Either of these approaches, or a hybrid implementation as in [18], could indeed be implemented outside the two-layer framework and would effectively compensate for the friction at the master side.

At the slave side however, only model-based feedforward control can be implemented adequately outside the two-layer framework. A sufficiently accurate model might not be derivable to implement in a feedforward controller. However, if the derived model underestimates the physical friction, it can still be used in the *Passivity Layer* to reduce the net passivity of the system that is enforced by the TDP algorithm. This will not increase the position tracking performance of the slave device, but will prevent the force reflection to the user to be adversely influenced by the TDP algorithm. Possible adaptive position control techniques that could be applied are necessarily implemented in the *Transparency Layer*. Thus friction compensation should also be implemented in the *Passivity Layer*.

7. Conclusions and future work

In this paper a method is proposed and experimentally validated to improve the transparency obtainable with TDP algorithms when applied to devices with non-negligible mechanical friction. The friction in the slave device was recognized as a major limiting factor in the obtainable transparency with TDP algorithms as it forms a continuous drain of energy that needs to be compensated by the user. Extending the energy balance monitored by the TDP algorithm to incorporate the device friction decreases the net passivity enforced by the TDP algorithm of the telemanipulation system. This decreases the influence that the TDP algorithm exerts on the commands computed by the bilateral control algorithm in the *Transparency Layer*. Thus the obtainable transparency with the telemanipulation system as a whole is increased. The desired stability properties of the TDP algorithm are maintained as long as the implemented friction model underestimates the physical friction. The results in this paper were specific to the two-layer framework, but the approach is applicable to any TDP algorithm, e.g. [7,8].

Future work will focus on further validation of the proposed approach. Experiments with devices containing multiple degrees of freedom and friction effects other than mere coulomb friction have to be conducted. The use of online friction identification methods, e.g. observer-based and delineated feature identification methods, will be explored.

Imperfections in the test setup (mechanical play and measurement noise) thus far prevented the use of a friction compensation method in the *Transparency Layer*. Compensation methods that are robust with respect to these imperfections will be investigated and/or mechanical parts of the setup itself will be redesigned and fabricated.

The practical significance of the proposed friction compensation technique also needs to be demonstrated. To that end human subject studies will need to be performed focusing on the performance with respect to tasks such as stiffness discrimination. A performance increase with respect to this task is expected when the proposed friction compensation is implemented.

Extending the energy balance in the TDP algorithm can also be used to increase the complimentarity of TDP algorithms with passivity based design approaches in the frequency domain, e.g. Absolute Stability [34] and Bounded Environment Passivity [35]. Preliminary results with a combination of both types of approaches are reported by Franken et al. [36].

Acknowledgements

The authors thank Roel Metz and Marcel Schwirtz for their contribution in the realization of the experimental test setup.

References

[1] Lawrence D. Stability and transparency in bilateral teleoperation. IEEE Trans Rob Autom 1993;9(5):624–37.
[2] Kim J, Chang PH, Park HS. Transparent teleoperation using two-channel control architectures. Proc IEEE/RSJ Int Conf Intel Robots Syst 2005:1953–60.
[3] Goethals P, De Gersem G, Sette M, Reynaerts D. Accurate haptic teleoperation on soft tissues through slave friction compensation by impedance reflection. Proc World Haptics 2007:458–63.
[4] Lee D, Li PY. Passive bilateral control and tool dynamics rendering for nonlinear mechanical teleoperators. IEEE Trans Robot 2005;21(5):936–51.
[5] Hokayem P, Spong M. Bilateral teleoperation: an historical survey. Automatica 2006;42:2035–57.
[6] Hogan N. Controlling impedance at the man/machine interface. Proc IEEE Int Conf Robot Autom 1989:1626–31.
[7] Ryu J-H, Kwon D-S, Hannaford B. Stable teleoperation with time-domain passivity control. IEEE Trans Robot Autom 2004;20(2):365–73.
[8] Ryu J-H, Artigas J, Preusche C. A passive bilateral control scheme for a teleoperator with time-varying communication delay. Mechatronics 2010;20:812–23.
[9] Kim J-P, Ryu J. Robustly stable haptic interaction control using an energy-bounding algorithm. Int J Robot Res 2010;29(6):666–79.
[10] Lee D, Huang K. Passive-set-position–modulation framework for interactive robotic systems. IEEE Trans Robot 2010;26(2):354–69.
[11] Franken M, Stramigioli S, Reilink R, Secchi C, Macchelli A. Bridging the gap between passivity and transparency. Robot Sci Syst 2009:281–8.

[12] De Gersem G, Van Brussel H. Influence of force disturbances on transparency in bilateral telemanipulation of soft environments. Proc IEEE Int Conf Robot Autom 2004:1227–32.
[13] Friedland B, Park Y-J. On adaptive friction compensation. IEEE Trans Autom Contr 1992;37(10):1609–12.
[14] Vedagarbha P, Dawson D, Feemster M. Tracking control of mechanical systems in the presence of nonlinear dynamic friction effects. IEEE Trans Contr Syst Tech 1999;7(4):446–56.
[15] Feemster M, Vedagarbha P, Dawson DM, Haste D. Adaptive control techniques for friction compensation. Mechatronics 1999;9(2):125–45.
[16] Tomei P. Robust adaptive friction compensation for tracking control of robot manipulators. IEEE Trans Autom Contr 2000;45(11):2164–9.
[17] Kwon D-S, Woo K. Control of the haptic interface with friction compensation and its performance evaluation. Proc IEEE/RSJ Int Conf Intel Robots Syst 2000:955–60.
[18] Bernstein L, Lawrence D, Pao L. Friction modeling and compensation for haptic interfaces. Proc World Haptics 2005:290–5.
[19] Ando N, Szemes P, Korondi P, Hashimoto H. Friction compensation for 6dof cartesian coordinate haptic interface. Proc IEEE/RSJ Int Conf Intel Robots Syst 2002:2893–8.
[20] Liu G, Goldenberg AA, Zhang Y. Precise slow motion control of a direct-drive robot arm with velocity estimation and friction compensation. Mechatronics 2004;14(7):821–34.
[21] Mahvash M, Okamura AM. Friction compensation for enhancing transparency of a teleoperator with compliant transmission. IEEE Trans Robot 2007;23(6):1240–6.
[22] Khayati K, Bigras P, Dessaint L-A. Lugre model-based friction compensation and positioning control for a pneumatic actuator using multi-objective output-feedback control via lmi optimization. Mechatronics 2009;19(4):535–47.
[23] Armstrong-Helouvry B, Dupont P, Canudas de Wit C. A survey of models, analysis tools, and compensation methods for the control of machines with friction. Automatica (Oxf) 1994;30(7):1083–138.
[24] Bona B, Indri M. Friction compensation in robotics: an overview. Proc IEEE Conf Decis Control 2005:4360–7.
[25] Bi D, Li Y, Tso S, Wang G. Friction modeling and compensation for haptic display based on support vector machine. IEEE Trans Ind Electr 2004; 51(2):491–500.
[26] Monfaredi R, Razi K, Ghydari SS, Rezaei SM. Achieving high transparency in bilateral teleoperation using stiffness observer for passivity control. Proc IEEE/RSJ Int Conf Intel Robots Syst 2006:1686–91.
[27] Love LJ, Book W. Force reflecting teleoperation with adaptive impedance control. IEEE Trans Syst Man Cybern B Cybern 2004;34(1):159–65.
[28] Franken M, Misra S, Stramigioli S. Friction compensation in energy-based bilateral telemanipulation. Proc IEEE/RSJ Int Conf Intel Robots Syst 2010:5264–9.
[29] Franken M, Stramigioli S, Misra S, Secchi C, Macchelli A. Bilateral telemanipulation with time delays: a two-layer approach combining passivity and transparency. IEEE Trans Robot, in preparation.
[30] Suraneni S, Kar I, Murthy OR, Bhatt R. Adaptive stick-slip friction and backlash compensation using dynamic fuzzy logic system. Appl Soft Comput 2005;6(1):26–37.
[31] Hannaford B, Ryu J-H, Kwon D-S, Kim YS, Song J-B. Testing time domain passivity control of haptic enabled systems. In: 8th Int Symp Exp Robot.
[32] Artigas J, Vilanova J, Preusche C, Hirzinger G. Time domain passivity control-based telepresence with time delay. Proc IEEE/RSJ Int Conf Intel Robots Syst 2006:4205–10.
[33] Controllab Products B.V., 20-sim version 4.1., 2010. <http://www.20sim.com/>.
[34] Hashtrudi-Zaad K, Salcudean SE. Analysis of control architectures for teleoperation systems with impedance/admittance master and slave manipulators. Int J Robot Res 2001;20(6):419–45.
[35] Willaert B, Corteville B, Reynaerts D, Van Brussel H, Vander Poorten EB. A mechatronic analysis of the classical position-force controller based on bounded environment passivity. Int J Robot Res 2010:1–18.
[36] Franken M,Willaert B, Misra S, Stramigioli S. Bilateral telemanipulation: improving the complimentarity of the frequency- and time-domain passivity approaches. Proc IEEE Int Conf Robot Autom, in press.